RASĀYAN *J. Chem.*
Vol. 19 | No. 1 | 449-456 | January-March | 2026
ISSN: 0974-1496 | e-ISSN: 0976-0083 | CODEN: RJCABP
http://www.rasayanjournal.com
http://www.rasayanjournal.co.in

DEVELOPMENT OF POLYPYRROLE-YTTRIA STABILIZED ZIRCONIA HYBRID CATALYST FOR ENHANCED PHOTODEGRADATION OF CONGO RED DYE

H. Gujjaramma[1], K. Gurushantha[2,✉], B.S. Krishna[1,3], S. Shashidhar[4], B. Prashanth[5], S. Meena[6], and K. V. Brungesh[7]

[1]Department of Chemistry, Cambridge Institute of Technology, North Campus, Bangalore 562110, India
[2]Department of Chemistry, M.S Ramaiah Institute of Technology, Bengaluru- 560054, India, Visvesvaraya Technological University, Belagavi, Karnataka, India
[3]Department of Chemistry, Harsha Institute of Technology, Bengaluru- 562123, India,
[4]Department of Chemistry, New Horizon College of Engineering, Bengaluru- 560103, India
[5]Department of Mechanical Engineering, Cambridge Institute of Technology, North Campus, Bangalore 562110, India
[6]Department of Chemistry, Dayananda Sagar College of Engineering, Bengaluru- 560111, India
[7]Department of Chemistry, Acharya Institute of Technology, Bengaluru- 560107, India
✉Corresponding author: gurushashimeena1986@gmail.com

ABSTRACT

Synergistic effects from combining different materials can produce and enhance nanomaterials' qualities, which are advantageous for raising the effectiveness of photocatalytic processes. In this current work, polymer-based hybrid composite photocatalysts are mainly synthesised of polypyrrole @ yttria stabilised zirconia (1.05,1:1,1:2) by cost effective combustion method, using *urea* as fuel. The composite perhaps changed the size and morphology of the yttria-stabilised zirconia, as evident from the results of XRD and SEM analysis. The XRD results support the crystal size ranging from 30 nm to 49 nm. The band gap varies from 3.2eV to 2.7 eV, which strongly affects the photocatalytic efficiency of Congo red dye in the UV and visible light. The PPy/YSZ -2 shows 99% under UV light and 89% in Visible light at pH 7.

Keywords: Polypyrrole @ Yttria Stabilised Zirconia, Photocatalyst, Congo Red, Degradation of Dye.
RASĀYAN *J. Chem.*, Vol. 19, No.1, 2026

INTRODUCTION

Synthetic dyes such as Congo Red (CR) are extensively used in the textile, paper, plastic, and leather industries due to their vivid colouration and chemical stability. It is a azo dye with -N=N- chromophores and sulfonate functional groups, being highly chemically stable and resistant to standard treatment procedures, posing significant environmental and health hazards.[1,2] Congo Red is particularly notorious for its toxicity, carcinogenicity, and potential to cause allergic reactions. When discharged into water bodies, it reduces light penetration, interferes with aquatic photosynthesis, and deteriorates water quality. Therefore, the removal or degradation of Congo Red from industrial effluents has become a critical research priority.[3,4] Numerous methods, including adsorption, photocatalysis, advanced oxidation processes, and membrane filtration, have been explored to address this challenge. Among these, nanomaterial (NM)-assisted adsorption and photocatalytic degradation are considered highly efficient, sustainable, and cost-effective approaches. Mainly, Semiconductor-based nanomaterials have emerged as an environmentally friendly choice for photocatalytic degradation to remove dyes.[5] This method uses the light energy to activate the photocatalyst to produce electron-hole pairs, which undergo oxidation and reduction reactions, finally degrading the dye to harmless end products, like CO_2 and H_2O. One of the most important research directions in environmental nanotechnology is therefore to develop effective, visible-light responsive photocatalysts with higher charge separation and surface activity.[6] Though many metal oxides, like ZnO, Cu@ZnO, Y_2O_3@ ZnO, Cr/ZnO, and TiO_2/ZnO, have unique properties in dye degradation.[2,7] all have ended with certain limitations. Zirconia's exceptional mechanical, electrical,

http://doi.org/10.31788/RJC.2026.1919602

thermal, and optical qualities make it one of the most significant ceramic materials. It is renowned for its high dielectric constant, optical transparency, excellent chemical and photochemical stability, and exceptional toughness.[8] In this regard Yttria-stabilized zirconia (YSZ) is a type of ceramic material that is frequently used due to its special qualities. It successfully withstands deterioration because of its high mechanical strength, hardness, high chemical resistance and temperature stability.[9] Because of its well-known superior oxide ion conductivity over 800°C, chemical and thermodynamic stability, and mechanical robustness, 8mol% yttria stabilised zirconia (8YSZ) has received more attention.[10] A wide range of photochemical activities can be stimulated by the bandgap energy of several compounds. Yttria stabilised Zirconia (YSZ), 3.2eV band gap in an N-type semiconductor, is a common building block for solid oxide fuel cell electrolytes, gas sensors, optical devices, cosmetics, ceramics, and textiles.[11] Because of its conjugated structure, polypyrrole (Ppy) is a highly favoured conductive polymer. It exhibits excellent photo-induced charge separation and outstanding electron transport capabilities. Electrochemical and chemical approaches have made it simple to produce Ppy. Ppy composite polymer photocatalysts have been employed in the literature for the photocatalytic degradation of organic dyes.[12,13,14] A good way to enhance the physicochemical and electrical characteristics of bare ZrO_2 is to mix it with conducting polymers or carbon-based materials to increase its catalytic qualities and solar cell performance. Synergistic effects from combining different materials can produce and enhance nanomaterials' qualities, which are advantageous for raising the effectiveness of photocatalytic processes. In the case of polymer-based hybrid photocatalysts, the synergistic impact resulting from the combination of distinct ingredients is readily apparent.[15,16] Solution combustion synthesis (SCS) allows for the quick formation of certain metastable phases, making the preparation of new materials simple. It is simple to create NMs with a high active surface in heterogeneous materials, which is advantageous for charge carrier separation and transfer.[9] Due to overcome certain limitations of other metal oxides and to achieve the novel polymer-based NM, this work focused on the synthesis of polypyrrole @ yttria stabilised zirconia for the photocatalytic degradation of CR dye.

EXPERIMENTAL

Materials Used

Every reagent used in this experiment was analytical grade and used straight away, without additional purification. Pyrrole 98% (NR CHEM), Ferric chloride ($FeCl_3$) 98% (Molychem), Ethanol (Nice Chemicals Pvt. Ltd), Yttrium nitrate [$Y(NO_3)_3.6H_2O$] (Loba chemie pvt.ltd), Zirconyl nitrate [$ZrO(NO_3)_2.xH_2O$(Hemedia), Urea [NH_2CONH_2] and Glycine [NH_2CH_2COOH] (Thomas baker lab grade).

Synthesis of PPy/YSZ Composite

Yttria stabilised zirconia (YSZ) nanocrystalline powders having 8mol% Y_2O_3 were synthesised using a solution combustion technique by dissolving the stoichiometric quantity of nitrate salts in deionised water, separate solutions of yttrium nitrate and zirconyl nitrate hydrate were prepared, and urea was used as fuel. The mixture was placed in a magnetic stirrer and placed into the preheated muffle furnace at 450 ^{0}C. The solutions start boiling, and a gel-like compound formed then fuel catches fire nitrates undergo degradation by releasing an enormous amount of gasses and white foamy powder was formed. The final powder was finely ground before being sintered at 180 ^{0}C at 3hours. Using $FeCl_3$ as an oxidant, pyrrole was oxidised in an aqueous medium to produce polypyrrole and polypyrrole/YSZ nanocomposites. 50 millilitres of pure water were used to dissolve 0.25milliliter of pyrrole. Next, a dropwise addition of a ferric chloride(0.05ml) solution in 50 mL of distilled water was made to the pyrrole aqueous suspension. A black-colored slurry formed as a result of the reaction mixture being continually agitated for roughly four hours. The resulting product was filtered, repeatedly cleaned with distilled water and then ethanol, dried for 24 hours at 60 °C in an air oven, and then kept in a desiccator for additional testing. Similarly, the previously mentioned procedure was used to create PPy/8YSZ composites, and the reaction mixture was supplemented with ultrasonicated 8YSZ nanoparticles (50 mg in 50 mL). After being prepared, the materials were dried, cleaned, ground into a fine powder, and kept in a desiccator for additional examination. The resulting materials, which contained 0.5:1, 1:1and 2:1 Polypyrrole of w/w in the reaction mixture, were designated as PPy, PPy/YSZ-1, PPy/YSZ-2, and PPy/YSZ-3, respectively.

RESULTS AND DISCUSSIONS

Powder X-Ray Diffraction Studies

A characteristic wide peak with a value between 22^0 and 29^0 may be seen in Fig.-1, which shows that the synthesised polypyrrole (PPY) was amorphous in nature. The YSZ particles are linked to sharp diffraction peaks at 30.2, 35, 50.4, 59.97, 62.8, and 74, which may be indexed as the crystalline structure planes (111), (200), (220), (311), (222), and (400).

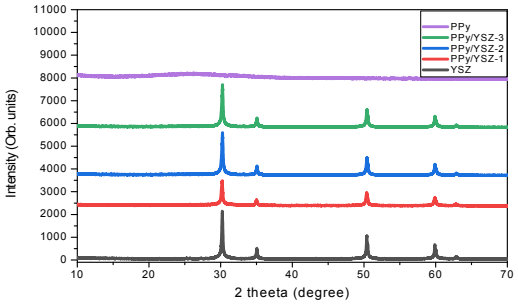

Fig.-1: XRD Studies of YSZ, PPy/YSZ-1, PPy/YSZ-2, PPy/YSZ-3 and PPy

Table-1: Estimated Crystallite Size, Surface Factor, Dislocation Density and Stress of PPy/YSZ Composites

Sample	Crystallite size(nm) by Scheer's method	Micro strain(ε) x 10^{-3}	Surface factor	Dislocation density(δ)(10^{15} lines per m^2)	Stress (σ)
PPy/YSZ-1	49.35	0.06934	0.4112	0.41	7.29
PPy/YSZ-2	47.57	0.07386	0.4585	0.46	7.76
PPy/YSZ-3	46.98	0.08017	0.4677	0.49	7.99
YSZ	30.65	0.1273	0.6521	1.49	6.30

It is possible to clearly identify the YSZ samples has face-centered cubic (fcc) structure using JCPDS Card No. 48-0224. Despite having wide bases, all PPy/YSZ peaks match the JCPDS data for YSZ material.[17] Table-1 shows the average crystallite size, microstrain, surface factor, dislocation density and stress.

Morphological Studies: SEM and EDAX

The micrographs of the PPy/YSZ-2 nanoparticles are shown in images Fig.-2a and b. It shows that the non-uniform distribution and nearly similar particle size are present. Agglomeration occurs to the same degree in PPy/YSZ-2 nanocomposites, but globular particles are still easily visible. The PPy/YSZ nanocomposites were discovered to have a diameter of 46.98 nm. Because PPy is coated on the YSZ surface. EDX Spectrum was used to determine the PPy/YSZ-2 nanocomposite's elemental composition. Y, Zr, carbon, nitrogen, and oxygen are the main constituents of the nanocomposites. PPy is mostly linked to Fe, C, N, and O. The formation of the PPy/YSZ nanocomposite was demonstrated by these morphological investigations, as shown in the Fig.-2b

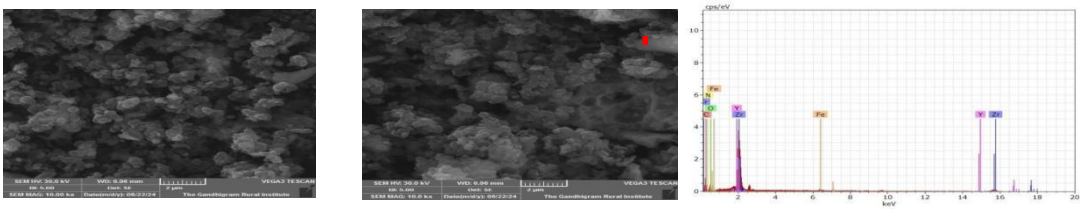

Fig.-2: a and b SEM Images of PPy/YSZ-2 Composite and C. EDAX of PPy/YSZ-2

FTIR

The FT-IR spectra of PPy, YSZ, PPy/YSZ-1, PPy/YSZ-2, and PPy/YSZ-3 are shown in Fig.-3a. In the Pyrrole ring, the stretching vibrations of C=C and C–C are responsible for the band at 1558 cm^{-1} and the weak band at 1468 cm^{-1}. In planar deformation modes, the C-H is represented by the absorption at

1284cm^{-1}. PPy exhibits the distinctive C–N and C–H stretching vibrations of Pyrrole in the infrared spectra, at 1159 cm^{-1} and 1031cm^{-1}, respectively.[17] The bands seen at 1004 and 676cm^{-1} may be attributed to the polymer's N–H vibrations and out-of-plane ring deformation. The bands at 2907cm^{-1}, 1558cm^{-1} and 1159 cm^{-1} are attributed to the pyrrole ring's N-H bending vibration of C=C and C-Cis, with the strong C-H stretch, strong C-H stretch, with C-N stretch, which supports the development of PPy.

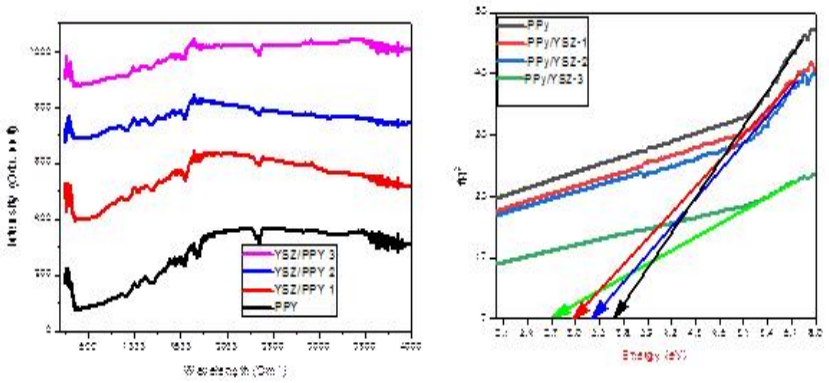

Fig.-3a: FTIR Spectra of PPy/YSZ-1, PPy/YSZ-2, PPy/YSZ-3 and PPy b. Energy Band Gap of PPy and PPy/YSZ Composites

Optical Studies

The band gaps of the synthesised materials were significantly influenced by their electrical structure, which was connected to their photovoltaic absorption capability. For PPy, PPy/YSZ-1, PPy/YSZ-2 and PPy/YSZ-3, the energy band gap estimates were 3.5, 2.9, 3.2 and 2.7 eV, respectively, as shown in Fig.-3b. In all cases, the Eg dropped as the concentration of YSZ ions increased from PPy, PPy/YSZ-1, PPy/YSZ-2 and PPY/YSZ-3, the space between bands dropped from 3.5 to 2.7 eV.

Photocatalytic Studies

Using a Wolfram (visible light) and an assortment of closed equipment 125W medium-pressure mercury lamp (UV light source), the dye photo-decolourisation was carried out in a batch experiment. UV and visible light were applied to a 100ml solution that contained 5ppm Congo red dye and 20mg of PPy/YSZ composite in different ratios for 90 minutes while being stirred continuously. The absorbance of the solution from the photo-decolourisation process, which was separated by ultra-centrifugation, was assessed with a UV-visible spectrophotometer that was configured to 497nm. To investigate the dye strength that remained in the solution, the absorbance that was then measured was interpolated into the corresponding standard curve. The following formula was used to determine the percentage of dye photo-decolourisation. Photo-Decolourisation ability (%) = $[A_O\text{-}A_t/A_t]$ where Ao is the first quantity of used dye and $A_{t\ is}$ the quantity of undetected dye in the mixture.

Effect of Catalyst

Understanding the availability of the catalyst's active sites requires research on catalyst dosage for the decolourisation process. The effect of dosage was examined by various catalyst ratios between PPy/YSZ-1, PPy/YSZ-2 and PPy/YSZ-3, which is shown in the Table-2, respectively.

Table-2: Percentage Degradation and Rate Constant of Polypyrrole Blended (0.5,1&2)/YSZ Composite

S. No.	Catalyst	Under ultraviolet light		Under visible light	
		% Degradation	Rate	% Degradation	Rate
1	PPy/YSZ-1	55.81	0.007532	38.93	0.004689
2	PPy/YSZ-2	99.36	0.047296	89.18	0.023897
3	PPy/YSZ-3	58.18	0.010091	80.77	0.017077

According to the study, the proportion of CR dye decolourisation decreases as the catalyst dosage is increased from PPy/YSZ-1 to PPy/YSZ-2, resulting in higher degradation efficiencies. Increasing the dosage of PPy decreases the degradation efficiency shown in the Fig.-4 a-d. The catalyst's decolourisation effectiveness rises as a result of the increased number of active sites on its outside that are essential for

the effective deposition of dye molecules[18], and its maximum electrical conductivity and lowest Eg value are responsible for this.

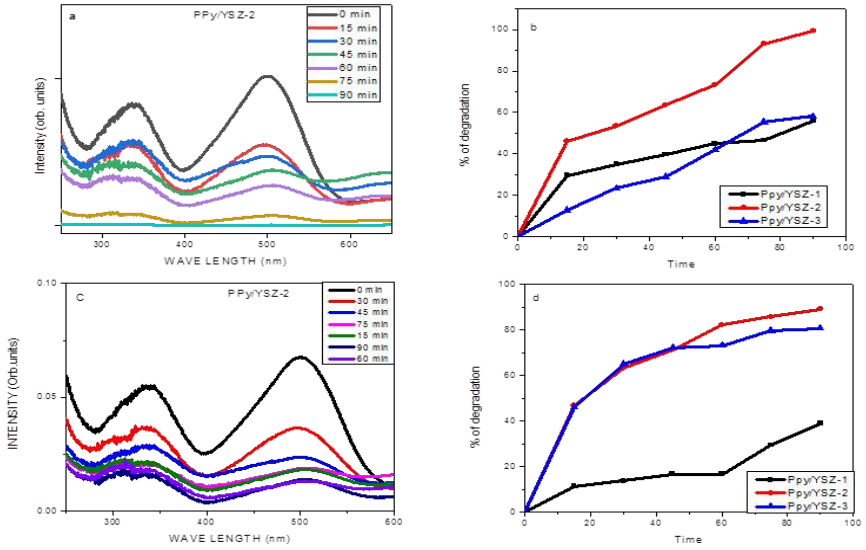

Fig.-4: (A) Photocatalytic Activity of CR Dye Under UV Light by PPy/YSZ-2 and (B) % Degradation under UV Light, and (C) Photocatalytic Activity of CR Dye Under Visible Light by PPy/YSZ-2 and (D) % Degradation under Visible Light

An electron moves between the conduction band and the valence band when PPy/YSZ-1 is exposed to UV and visible radiation. Because of its great electrical conductivity, this photo-generated charge has a large transfer capacity. The creation of nanocomposites is often two ways to increase the catalyst's photocatalytic activity. Polymer/metal or polymer/metal oxide nanocomposites' high photocatalytic activity is dependent on the blended comosite uniform dispersion of the blended composite within the polymer. As the Once the ratio reaches PPy/YSZ-3, the proportion of decolourisation decreases because the solution becomes more turbid, preventing light penetration and effectively reducing photon absorption[19], and the homogenous distribution of YSZ becomes skewed, and YSZ agglomerations may result. A consequent decline in photocatalytic activity is noted.[13] When a different blending ratio of PPy/YSZ is added, and the dye is exposed to an artificial UV and Visible lamp for 90 minutes, the percentage of Congo red dye degradation is 99% and 89%. The photocatalytic procedure employing PPy/YSZ composite catalyst powder and the wavelength and intensity of the UV light source have an impact on the dye degradation in aqueous solution. This is due to the fact that artificial UV irradiation is more consistent than sunlight, which can result in more effective dye degradation.[19]

pH Effect

pH has a significant part in dye degradation research, so to examine how pH affects degradation rate, dye degradation experiments were conducted at various pH levels (pH 2, pH 4, pH 6, pH 8 and pH 10) by adding either HCl or NaOH given in the Table-3. After adjusting the pH to 2, we observed that the protonation-induced π-π^* transition of the azo group, shifting to a higher wavelength(497nm), caused the colour of the Congo red mixture to change from red to blue. Protonation of CR may occur in the amino or azo nitrogen since it comprises four nitrogen atoms that could be protonation sites. Dye contains four nitrogen atoms that may be potential protonation sites; protonation of CR may occur in the amino or azo nitrogen.[2] As can be seen in Fig.-5 a-f, the degradation rate decreased when the CR solutions' pH was raised from 2 to 6. When the reaction pH is greater than the basic pH, the anionic character of the CR dye, which has two sulphonic groups that are easily ionised in acidic conditions to generate a soluble CR anion, occurs.[2,12] We saw 99% deterioration in 90 minutes at pH 7 when we conducted the pH investigation at several pH values given in the Table-3, such as 2, 4, 6, 8 and 10. We do not desire this kind of self-ionisation. In contrast, 90% degradation was attained in 90 minutes at pH 6. We have therefore conducted more research on the beginning dye strength, and at pH 6, a change in the quantity of catalyst. Because of

the high proton concentration, the photodegradation process is slowed down in acidic solutions with a pH below 6.[20] As a result, the percentage of degrading efficiency was reduced. In addition, the presence of hydroxyl ions neutralises the induced acidic end products generated by the photodegradation reaction in alkaline environments with pH values greater than 8. The inability of the dye molecules to reach the catalyst surface causes a drop in the initial rate in alkaline solutions, which leads to the best pH among those tested appearing to be neutral.[3,21,22]

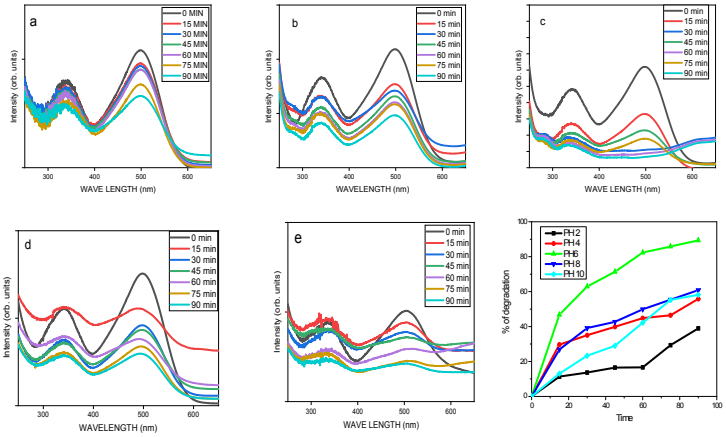

Fig.-5: absorbance Graphs of Congo red Dye using PPy/YSZ-2 Composites at (a)pH2, (b)pH4, (c) pH6, (d) pH8, (e) pH10 and (f) % Degradation

Photocatalytic Mechanism

When photocatalyst particles suspended in an aqueous solution are exposed to light with energy equal to or greater than their bandgap energy, they create valence band holes (h+) and electrons (e-) in the conduction band. The photogenerated electrons have the ability to convert the dissolved organic dye molecules to the superoxide radical anion, $O^{2\bullet}$. In addition to oxidising the organic dye molecules to produce oxidised species, the light produced hole can use OH or H_2O to react to change them into the hydroxyl radical, OH•. The photocatalytic breakdown of azo dye molecules is said to be significantly aided by the resultant $O^{2\bullet}$ and $OH^{\bullet}$ radicals. Most azo dye molecules can be oxidised to less hazardous compounds like H_2O and CO_2 by the $O^{2\bullet}$, $OH^{\bullet}$, and $HO^{2\bullet}$ radicals that are subsequently produced.

Table-3: Percentage of Degradation with Different pH of PPy/YSZ-2 under UV Light

S. No.	pH	% Degradation	Rate
1	2	38.93	0.004689
2	4	55.81	0.007526
3	6	89.35	0.024066
4	8	60.82	0.009506
5	10	58.19	0.010067

The following can be used to express the potential reactions that photocatalytic oxidation may cause at the surface of the semiconductor photocatalyst PPy@8YSZ.[24-25]

$$PPy@8YSZ + h\upsilon \rightarrow e^- + h^+ \quad (3)$$

$$e^- + O_2 \rightarrow O_2^{-\bullet} \quad (4)$$

$$h^+ + H_2O \rightarrow \bullet OH \quad (5)$$

$$h^+ + O_2^{-\bullet} + \bullet OH + Dye \rightarrow \text{degraded products} \quad (6)$$

CONCLUSION

The work showed success in the synthesis of polypyrrole @ yttria stabilised zirconia (PPy/YSZ-1, PPy/YSZ-2 and PPy/YSZ-3), which are polymer-based hybrid composite photocatalysts by the combustion method using *urea* as fuel. The PPy/YSZ formation was confirmed by XRD. The amorphous morphology of the sample was justified from the SEM images, which support photocatalytic applications.

The band gap of PPy/YSZ composites is from 3.2 to 2.7 eV. The toxic Congo red dye was successfully degraded under UV light and Visible by the PPy/YSZ samples. At pH 7, the sample PPy/YSZ-2 shows 99% degradation in UV light and 89% in visible light. The photocatalytic procedure employing the PPy/YSZ photocatalyst shows that light has an impact on the dye degradation in aqueous solution. The efficiency of degradation under UV light is better than sunlight, which could be due to the fact that artificial UV irradiation is more consistent than sunlight.

CONFLICT OF INTERESTS

The authors declare that there is no conflict of interest.

AUTHORS CONTRIBUTIONS

The present work is related to *SDG-6: Clean Water and Sanitization.* All the authors contributed significantly to this manuscript, participated in reviewing/editing and approved the final draft for publication. The research profile of the authors can be verified from their ORCID ids, given below:

H. Gujjaramma https://orcid.org/0009-0000-8426-9493
K. Gurushantha https://orcid.org/0000-0002-0759-9453
B. S. Krishna https://orcid.org/0000-0002-6609-3225
S. Shashidhar https://orcid.org/0000-0001-5745-7149
B. Prashanth https://orcid.org/0009-0004-0362-5329
S. Meena https://orcid.org/0000-0001-9979-8689
K. V. Brungesh https://orcid.org/0009-0002-2236-4959

Cite this article as: H. Gujjaramma *et al.*, *Rasayan J. Chem.*, 19(1), 449-456(2026), https://doi.org/10.31788/RJC.2026.1919602.

REFERENCES

1. J. S. Dhanaji, and R. S. Patil, *Journal of Water and Environmental Nanotechnology,* **7(2),** 170(2022), https://doi.org/10.22090/jwent.2022.02.005
2. B. O. Ujwala, J. J. Wu, A. M. Asiri, and S. Anandan, *ChemistrySelect*, **42(3),** 11851(2018), https://doi.org/10.1002/slct.201802303
3. N. Harun, M. Rahman, W. Kamarudin, Z. Irwan, A. Muhammud, N. Akhir, and M. Yaafar, *Journal of Fundamental and Applied Sciences*, **10(1S),** 832(2018), https://doi.org/10.4314/jfas.v10i1S
4. M. Shaban, M. R. Abukhadra, S. S. Ibrahim, and M.G. Shahien, *Applied Water Science*, **7**, 4743(2017), https://doi.org/10.1007/s13201-017-0637-y
5. H. H. Hassan, H. Traboulsi, R. K. Karnati, and E. M. Bakir, *Catalysts,* **12(3),** 248 (2022), https://doi.org/10.3390/catal12030248
6. A. Fuentes, Sara, R. Feria-Reyes, E. Ramos-Ramírez, Norma Gutiérrez-Ortega, and Gustavo Cruz-Jiménez, *Catalysts,* **11(2),** 211 (2021), https://doi.org/10.3390/catal11020211
7. S. Shashidhar, V. A. Shastry, K. Gurushantha, K. V. Brungesh, S. Meena, K. S. Anantharaju and G. K. Raghu, *Rasayan Journal of Chemistry*, **18(1),** 1(2025), http://doi.org/10.31788/RJC.2025.1819075
8. L. Ramakrishna, T. Ramakrishnappa, K. M. Girish, K. Suresh Kumar, *Next Materials,* **4,** 100193 (2024), https://doi.org/10.1016/j.nxmate.2024.100193
9. S. J. Kareem, A. M. Wurood, S. Abbas, and H. Al-Ethari, *Advances in Science and Technology. Research Journal,* **18(4),** 410(2024), https://doi.org/10.12913/22998624/189848
10. A. F. Abeer, S. B. H. Farid, and F. A. Hashim, *Engineering and Technology Journal*, **38(4A),** 491(2020), https://doi.org/10.30684/etj.v38i4A.351
11. H. Gujjaramma, B. S. Krishna, K. Gurushantha, S. Meena, G. Shobha, and G. K. Raghu, *Desalination and Water Treatment,* **317,** 100301 (2024), https://doi.org/10.1016/j.dwt.2024.100301

12. B. H. Taymaz, H. Kamiş, and Ö.Yoldaş, *Environmental Engineering Research,* **27(2),** 200638(2022), https://doi.org/10.4491/eer.2020.638
13. A. Parveen, and N. Surumbarkuzhali, *Inorganic Chemistry Communications,* **120,** 108153(2020), https://doi.org/10.1016/j.inoche.2020.108153
14. M. Sravanthi, and K. G. Manjunatha, *Materials Today: Proceedings,* **46,** 5964(2021), https://doi.org/10.1016/j.matpr.2020.11.762
15. J. N. Chandra, K. Kaur, N. Kumar, N. S. Bhandari, and A. Thakur, *Nano-Structures & Nano-Objects,* **25,** 100669(2021), https://doi.org/10.1016/j.nanoso.2021.100669
16. I. N. Venkat, J. A. Kher, and S. D. Bhame, *Journal of Water and Environmental Nanotechnology,* **8(4),** 334 (2023), https://doi.org/10.22090/jwent.2023.04.002
17. S. Sacchidanand, J. A. Kher, and M. V. Kulkarni, *Journal of Nanomedicine & Nanotechnology,* **6(5),** 1(2015), https://doi.org/10.4172/2157-7439.1000313
18. S. Supriya, and S. Sathish, *Inorganic and nano-metal chemistry,* **50(3),** 100(2020), https://doi.org/10.1080/24701556.2019.1661442
19. S. Ahmed, H. Teymourinia, A. Zarei, M. Timoumi, and A. Ramazan, *Iranian Journal of Catalysis,* **12(1),** 97(2022), https://doi.org/10.30495/ijc.2022.68962
20. H. A. Nurul, D. Amalia, and E. T. Wahyuni, *The Scientific World Journal,* **1,** (2022), https://doi.org/10.1155/2022/2613841
21. N. Falak, A. Imran, W. Ullah, K. Saeed, S. Ali, and M. N. Khan, *Iranian of chemistry and chemical engineering,* **41(8),** 2790(2022), https://doi.org/10.30492/ijcce.2021.522330.4499
22. A. M. Santhosh, K. Yogendra, K. M. Mahadevan, and N. Madhusudhana, *International Journal of Advance Research in Science and Engineering,* **6(7),** 51(2017), https://doi.org/10.26438/ijsrpas/v6i5.4856
23. M. N. Alshabanat, and M. M. AL-Anazy, *Journal of Chemistry,* **1**, (2018), https://doi.org/10.1155/2018/9651850
24. M. A. Alenizi, R. Kumar, M. Aslam, F. A. Alseroury, and M. A. Barakat, *Scientific Reports,* **9(1),** 12091(2019), https://doi.org/10.1038/s41598-019-48516-3
25. C. R. Michel, and A. H. Martínez-Preciado, *Open Ceramics,* **13,** 100336 (2023), https://doi.org/10.1016/j.oceram.2023.100336

[RJC-9602/2025]